Ab Initio Study of Nitromethane Deprotonation by $(OH)^-\cdot nH_2O$ Clusters

Dario Bekšic, Juan Bertrán,* and José M. Lluch

Departament de Química, Universitat Autònoma de Barcelona, 08193 Bellaterra, Barcelona, Spain

James T. Hynes

Department of Chemistry and Biochemistry, University of Colorado, Boulder, Colorado 80309-0215

Received: October 23, 1997; In Final Form: March 2, 1998

The deprotonation of nitromethane by $(OH)^-\cdot nH_2O$ clusters has been studied. Ab initio quantum chemistry calculations including electron correlation are used to determine the geometries, energetics, and natural bond orbital electronic populations of reactants, transition states, and products for the cases of $n = 0$ and $n = 2$. An analysis of the negative charge redistribution during the reactions is given. In particular, special attention is devoted to the evolution of the negative charge on carbon, which has been implicated in the past in the observed anomalous values of the Brønsted parameter in the reaction of interest, the so-called "nitroalkane anomaly". Finally, the deprotonation of nitromethane by $(OH)^-$ is compared with the analogous reaction involving acetonitrile; the results suggest that the high electron affinity of the NO_2 group is critical for the existence of the nitroalkane anomaly.

1. Introduction

Among proton-transfer reactions, which themselves are among the most fundamental processes in chemistry,[1−8] proton transfer from nitroalkanes has attracted particular attention due to its extraordinary kinetic properties, which have been explored both experimentally[10−13] and theoretically.[1,9,12−23] The present work presents ab initio quantum chemical calculations on one of the simplest members of this reaction class $NO_2CH_3 + (OH)^-\cdot(H_2O)_n \rightarrow (NO_2CH_2)^- + (n+1)H_2O$ for $n = 0$ and $n = 2$. Its goal is to provide microscopic insights on this reaction and also to examine the influence of microsolvation.

An important reason for the wide interest in proton transfer from nitroalkanes, alluded to above, is their behavior in the context of the Brønsted relation

$$\log k = \alpha \log K_a + \text{constant}$$

connecting the reaction rate constant k and the equilibrium constant K_a, with the proportionality constant α known as the Brønsted parameter. The Brønsted parameter, which measures the relative effects of, e.g., a substitution on the reaction rate and equilibrium, is generally expected to lie in the range between zero and one. In connection with the reaction energy profile,[24] under strongly exothermic conditions such that a reaction becomes diffusion-controlled, α should approach zero, while in the opposite limit of strongly endothermic reactions, α should approach unity. At a deeper level of interpretation which involves the Hammond postulate[25] connecting the energy profile to the transition state location, the Brønsted parameter would also be a measure of the transition state location, being small for reactant-like transition states and close to unity for the opposite case. These ideas have been the subject of much discussion and scrutiny.[1,9,11−19,27,28]

Nitroalkanes constitute an important exception to the aforementioned model, as the Brønsted parameter values outside of the postulated [0,1] interval have been observed.[11,12] This phenomenon has become known as the "nitroalkane anomaly", and it has been related in various ways to the idea that, as the reaction progresses, the negative charge accumulated on the carbon atom bonded with nitrogen is larger in the transition state than in the final products. A variety of explanations has been proposed in relation to the physical cause of the "anomaly" (for review, see Pross[15]), including the geometry relaxation as the reaction evolves toward the products,[11] the effects of solvation on charge delocalization,[9,14,26] and the effects of valence bond configuration mixing in the transition state.[15] The present study examines such features in terms of the results of quantum chemical calculations for the paradigm reactions above and aims to give some quantitative background for a more complete physical picture of the nitroalkane deprotonation reaction.

The fact that the anomalous Brønsted parameter values are usually absent in proton transfers from other carbon acids suggests that the "anomaly" may be directly related to the high electron affinity of the NO_2 radical and its influence on the intramolecular charge redistribution. This idea is tested in the final part of this work, where nitromethane is replaced by acetonitrile ($CNCH_3$), which itself has been widely studied, in particular in the context of deprotonations by anions, e.g., by F^- [50,51] or by hydrated $(OH)^-$.[52] Although we are unaware of experimental study of the Brønsted parameter for these deprotonations, the $CNCH_3$ case is an interesting one for both contrast and theoretical prediction.

After the present work was completed, an ab initio study of the gas-phase nitromethane to nitromethide anion proton-transfer identity reaction by Bernasconi and co-workers[23] has appeared, which has a focus (and reaction) different from the present work's attention to the microsolvation aspects of proton transfer from nitromethane.

2. Method of Calculation

Ab initio restricted Hartree−Fock (RHF)[29] calculations have been carried out using the split-valence 6-31+G** basis set,[30,31]

S1089-5639(97)03426-9 CCC: $15.00
Published on Web 05/07/1998

TABLE 1: Geometrical Parameters of NO_2CH_3 (Distances in Å, Angles in deg)[a]

method	6-31G*//6-31G* [b]	6-31+G**//6-31+G** [c]	MP2/6-31G*//MP2/6-31G* [d]	MP2/6-31+G**//MP2/6-31+G** [c]	exptl[e]
C−N distance	1.478, 1.479	1.481, 1.481	1.485, 1.486	1.489, 1.490	1.4855
N−O distance	1.192, 1.191/1.193	1.193, 1.192/1.193	1.240, 1.241/1.239	1.244, 1.243/1.244	1.2270
O−N−O angle	125.8, 125.3	125.6, 125.6	125.7, 125.8	125.5, 125.4	123.7
O−N−C angle	117.1, 117.7/116.5	117.2, 117.8/116.6		117.3, 118.0/116.6	
H(b)−C−N angle	108.0, 108.4	107.9, 108.1	107.8, 108.1	107.7, 108.0	
H(a)−C−N angle	106.5, 107.0	106.4, 106.9	107.1, 107.3	106.9, 107.2	106.4

[a] The first number refers to the staggered conformation; the second number refers to the eclipsed one. [b] From ref 36. [c] This work. [d] From ref 37. [e] From X-ray diffraction experiment; ref 40.

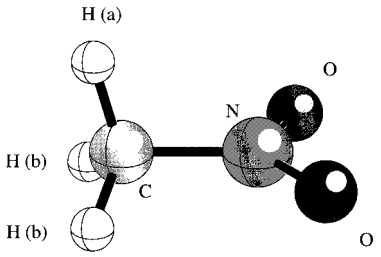

Figure 1. Nitromethane equilibrium geometry, staggered conformation.

which includes p and d polarization orbitals on the hydrogen and heavy atoms, respectively, and a diffuse sp shell on the heavy atoms. Diffuse functions[32] are needed for an appropriate representation of charge distributions in anionic species. Electron correlation energy has been included by means of second-order Möller−Plesset perturbation theory (MP2).[33] At both levels of calculation, natural bond orbital (NBO) electronic population analysis has been carried out with the corresponding electronic density, while full geometry optimization and direct location of stationary points have been done with the Schlegel gradient optimization algorithm.[34] The characterization of both kinds of stationary points, minima or transition states, has been carried out by diagonalizing the corresponding Hessian matrixes and seeking zero or one negative eigenvalues, respectively. The calculations have been performed with the GAUSSIAN 94 software package.[35]

3. Structures of Nitromethane and Nitromethide Anion

The results obtained in this paper for NO_2CH_3 and the $(NO_2CH_2)^-$ anion can be compared with earlier theoretical[36,37] and experimental[38−40] work. Table 1 gives the results for nitromethane, in both of its stable conformations, "staggered" and "eclipsed". Good agreement is observed with earlier theoretical values.[23,36,37] The staggered conformation turns out to be the most stable and is shown by Figure 1; the eclipsed conformation differs from it by the methyl group being rotated around the C−N axis until one of its hydrogens falls into the nitro group plane. However, the energy difference between the two conformations is only about 0.03 kcal/mol at the MP2 level, so the two conformations are experimentally indistinguishable. This essentially degenerate character demonstrates that the role of possible hyperconjugation between the orbitals of the methyl group hydrogens and the nitro group oxygens is extremely feeble. Finally, the double values cited in Table 1 for the N−O distance and the O−N−C angle in the eclipsed conformation stem from the fact that the two nitro group oxygens are not symmetric in this case.

The nitromethide, or $(NO_2CH_2)^-$ anion, is considered next. In principle, the anion can be obtained by removing one of the protons from the neutral species. In this connection, a two-step "thought experiment" was performed. The first step consisted of removing (a) the proton in the plane perpendicular to the nitro group plane (marked by (a) in Figure 1) or (b) one of the protons "below" the nitro group plane (marked by (b) in Figure 1), keeping the rest of the geometry "frozen" with all the interatomic lengths and angles corresponding to the staggered nitromethane. Single point calculations were performed for both these cases. The resulting energies show which mode of deprotonation is favorable (in this case removing the (a) proton), while the NBO populations indicate the redistribution of negative charge upon deprotonation. In a second step, the anion geometry was allowed to relax. The optimization yielded the energies of 11 and 27 kcal/mol below the "frozen" anion geometries with the (a) proton and the (b) proton removed, respectively, but still 367 kcal/mol above the neutral species at the MP2 level. The resulting anion geometry, which is essentially planar, is shown in Figure 2, while Table 2 contains the relevant NBO populations. It is evident from all the results that in the second relaxation step a double bond is being formed between carbon and nitrogen (a 10% decrease in internuclear distance at the MP2 level), but it remains somewhat larger than the typical double C−N bond length, while the NO_2 group bond lengths are stretched out due to the loss of the double N−O resonant bond character.

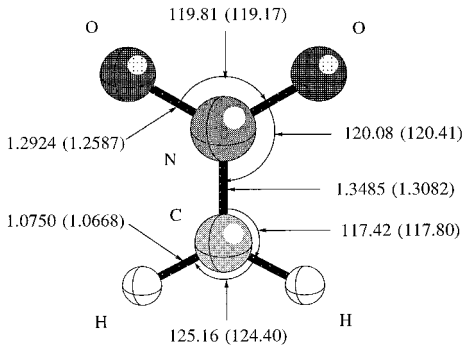

Figure 2. $(NO_2CH_2)^-$ anion MP2 optimized geometry, distances in angstroms, angles in degrees; RHF results in parentheses.

The charge distribution results in Table 2 indicate that the electronic charge redistribution accompanying the deprotonation has two different aspects: one is the accumulation of negative charge on the carbon atom and the nitro group at the moment the proton is removed and the other is a negative charge flow toward the nitro group stimulated by the geometrical relaxation. This trend is evident both including and excluding the electron correlation, but it must be remarked that it does *not* imply any "temporal" or "causal" behavior.

4. $NO_2CH_3 + (OH)^- \rightarrow (NO_2CH_2)^- + H_2O$ Reaction

As noted in the Introduction, the proton transfer from nitromethane to the hydroxide anion to produce the $(NO_2CH_2)^-$ anion and a water molecule can be considered as the most basic reaction for the "nitroalkane anomaly" studies. It involves the simplest of all nitroalkanes and has a marked exothermic character due to the presence of a base as strong as the $(OH)^-$ anion. This has made it a subject of various studies, both experimental[11−13] and theoretical.[1,9,15,19,22,23,28]

TABLE 2: Natural Orbital Populations of Nitromethane and Its Anion, in "Frozen" and Relaxed Geometries[a]

species	NO_2CH_3	$(NO_2CH_2)^-$ (a) frozen	$(NO_2CH_2)^-$ (b) (frozen)	$(NO_2CH_2)^-$ (optimized)
charge on carbon	−0.470, −0.511	−0.750, −0.683	−0.843, −0.819	−0.482, −0.489
charge on nitro group	-0.292, -0.257	-0.574, -0.656	-0.478, -0.520	-0.895, -0.893
av charge on hydrogen	0.254, 0.256	0.162, 0.170	0.161, 0.170	0.189, 0.191

[a] Charges in atomic units. First values are the RHF results, while second ones are MP2 results.

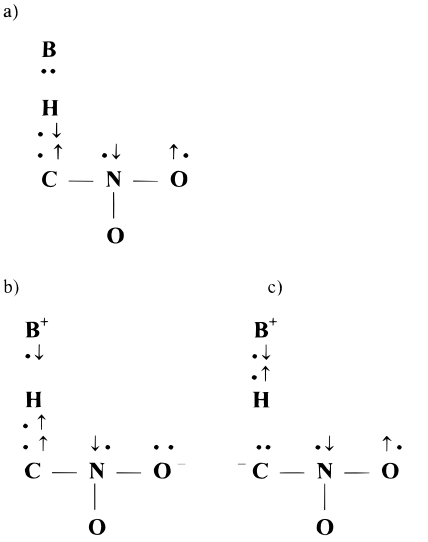

Figure 3. $NO_2CH_3 + (OH)^- \rightarrow (NO_2CH_2)^- + H_2O$ reaction valence bond configurations[15,44] for (a) reactant, (b) product, (b) and (c) transition state (configuration mixture).

Experiments in solution involving substitutions of the methyl group hydrogens[11] have determined the Brønsted parameter to be approximately equal to 1.7 for the $NO_2CH_3 + (OH)^- \rightarrow (NO_2CH_2)^- + H_2O$ reaction and to be −0.7 for the corresponding inverse reaction, i.e., both values lying out of the expected [0,1] range. Bordwell et al. have argued that this "anomalous" behavior is due to the sensitivity of the reaction not only to the position of the transition state but also to the considerable structural reorganization, a hypothesis later supported in other studies.[9]

As noted in the Introduction, many of the discussions of the nitroalkane anomaly invoke the importance of the presumed larger negative charge on the methyl carbon in the transition state as compared to its value in the product. A more recent valence bond theory description[15,44] of the nitromethane reaction with a general base has focused on the electronic charge reorganization along the reaction path, although somewhat qualitatively and without an explicit account of the geometry changes or solvation. This description provides a framework for comprehending both the possible origin of the different methyl carbon negative charges in the transition state and product and the resulting anomalous Brønsted behavior. In this model description, the reactant configuration, shown in Figure 3a, includes two electron bonding pairs (C−H and an N−O resonant π bond) on nitromethane and a separate one on the base. Two other configurations are included in the analysis: one of them, the product configuration, contains an accumulation of negative charge on the nitro group oxygens (Figure 3b), while on the other, intermediate, one the negative charge is concentrated on carbon (Figure 3c). The key feature of this analysis is that both of these configurations, especially the latter, make a contribution to the transition state. But as the reaction evolves toward the products, the former one becomes energetically more favorable, so in the product configuration the negative charge is accumulated on the nitro group oxygen atoms, rather than on the carbon atom: the participation of the intermediate configuration in the transition state, but not in the products, is the presumed cause of the anomalous Brønsted behavior.

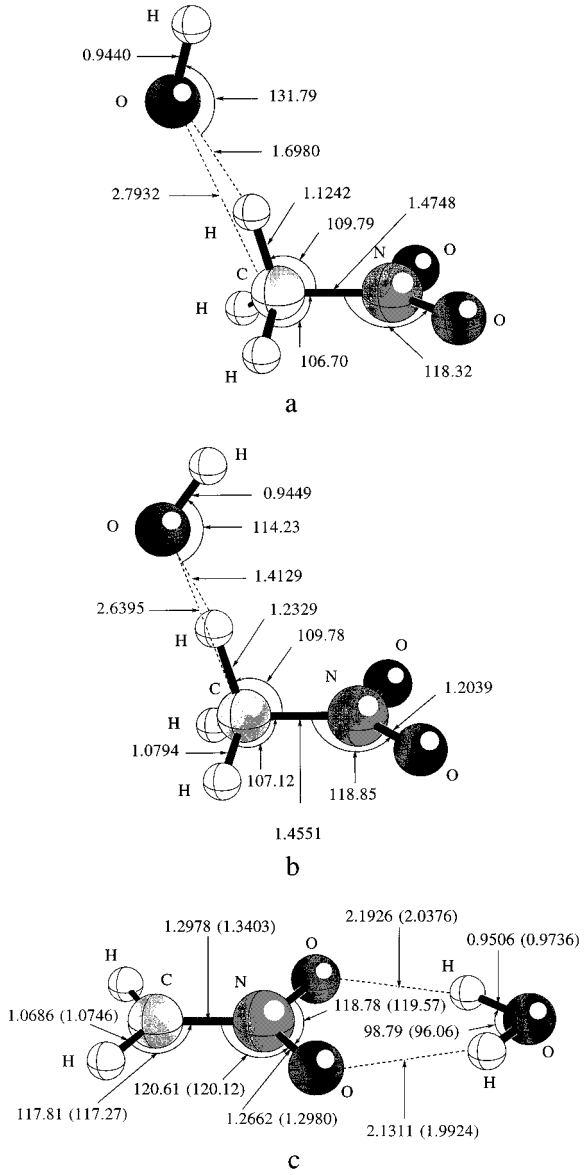

Figure 4. $NO_2CH_3 + (OH)^- \rightarrow (NO_2CH_2)^- + H_2O$ RHF geometries: (a) reactant, (b) transition state, and (c) product (MP2 results in parentheses); distances in angstroms, angles in degrees.

In the present study, ab initio quantum chemistry calculations were done first on the RHF level, to determine the geometries, energetics, and NBO populations of the stationary points of the reaction. The reactant was located starting by positioning the hydroxide anion close to the "(a)" hydrogen atom of staggered nitromethane; the resulting geometry is shown in Figure 4a. The transition state and product structures are shown in parts b and c of Figure 4, respectively. At this point it has to be remarked that, throughout this work, the terms "reactant" and "product" will be applied (unless stated otherwise) to structures in which the two fragments are forming a complex in the cluster, instead of being separated at infinite distance.

TABLE 3: Natural Orbital Population (in au) Data for the $NO_2CH_3 + (OH)^- \rightarrow (NO_2CH_2)^- + H_2O$ Reaction[a]

structure	reactant	transition state	product
charge on carbon	−0.521, −0.562	−0.586, −0.611	−0.424, −0.435
charge on NO_2	−0.373, −0.334	−0.421, −0.400	−0.941, −0.910
charge on $(OH)^-$	−0.931, −0.905	−0.838, −0.794	
charge on H to transfer	0.390, 0.360	0.427, 0.378	

[a] First values are the RHF results, while second ones are MP2 results.

The calculated transition state is, at least as far as geometry is concerned, clearly reactant-like, confirming the earlier predictions.[12] A Hessian matrix analysis, performed on the RHF level, shows that the reaction coordinate consists, at least close to the transition state, mainly of the transferring proton migration toward the hydroxide oxygen atom and the decrease in the H−O−H angle of the incipient water molecule product, with a small contribution of the C−N bond length reduction and other degrees of freedom. The reactant-like character of the transition state directly implies that the reaction should be clearly exothermic[25] and very fast in kinetic terms. Indeed, the exothermicity found here is approximately 30 kcal/mol. The energy barrier is, as expected, very low, less than 1 kcal/mol, which clearly indicates that the reaction must be fast, in accord with experimental observations.[41]

Next, with the above RHF optimized geometries as starting points, the calculations were repeated for the same reaction, but now including electron correlation via the MP2 algorithm. While the fully optimized product structure is quite similar to that obtained on the RHF level (Figure 4c), no reactant well could be detected on the MP2 level, and consequently no transition state can be defined. This is actually not so surprising, because the RHF energy barrier was already extremely low. Nonetheless, we will refer below to this point as the transition state, due to its identification at the RHF level.

The next important point to discuss is the variation along the reaction path of the NBO populations given in Table 3, indicating the electronic charge redistribution in the system. Since no reactant well was found on the MP2 level, the MP2 results for the reactant and the transition state are the NBO populations evaluated by using the MP2 densities, but with the RHF geometries. The overall exothermicity of the reaction is well expected because its net result in electrostatic terms is a considerable negative charge delocalization from a relatively small hydroxide anion to a much larger $(NO_2CH_2)^-$ anion. Examination of the Table 3 data shows that, while the transition state is formed, the electronic charge is transferred from the hydroxide (and to a lesser extent from the transferring proton) to both the carbon atom and the nitro group. As the reaction progresses toward the product, the incipient $(NO_2CH_2)^-$ anion relaxes toward its planar form, forming a double C−N bond (evidenced by the bond length decrease, quantitatively similar to the isolated molecule case, discussed in section 3), and the formed water migrates to solvate the anion (cf. Figure 4c); simultaneously, the negative charge is transferred toward the nitro group oxygen atoms, with the nitrogen atom basically acting as a spectator. As a consequence, the carbon negative charge at the transition state (−0.611 au) is greater than the one corresponding to the product (−0.435 au), in accord with the expectations discussed above.

5. $NO_2CH_3 + (OH)^-\cdot 2H_2O \rightarrow (NO_2CH_2)^- + 3H_2O$ Reaction

Of the different possibilities for including several water molecules in the nitromethane−hydroxide system, the most convenient one from the experimental point of view is that in which one would prepare a cluster consisting of the hydroxide anion coordinated with one or several water molecules, and then react it at low energy (thermal or less) with pure nitromethane. The presence of water molecules bound via hydrogen bonds to the hydroxide ion is expected to significantly modify the energy profile of the proton-transfer reaction. For example, since there is a strong ion−dipole interaction between the hydroxide ion and the waters, the energy of the reactant should be lowered and thus the contribution of the reactant to the reaction exothermicity should be reduced. In addition, the properties of the transition state and finally the geometry and charge distribution of the final product will be altered.

It is known[42,43] that up to three water molecules can form a stable cluster (single solvation shell) around the hydroxide anion, due to the fact that there are three pairs of electrons on its oxygen atom disposed to participate in hydrogen bonds. Therefore, the $(OH)^-\cdot 2H_2O$ cluster is a natural choice for the present work: two oxygen electron pairs are each coordinated with one water, and the remaining electron pair is left to accept the proton to be transferred from nitromethane.

As in section 3, the calculations were performed first on the RHF level and determined the geometry, energetics, and charge distribution of reactant, transition state, and product for the $NO_2CH_3 + (OH)^-\cdot 2H_2O \rightarrow (NO_2CH_2)^- + 3H_2O$ reaction. These structures are shown by parts a (reactant), b (transition state), and c (product) of Figure 5, with the relevant geometrical parameters indicated in parentheses. The NBO population data are presented in Table 4.

A comparison of these RHF results shows that this reaction is in its general features similar to the corresponding reaction with $n = 0$, studied in Section 4. In particular, it is still exothermic and the transition state is still rather reactant-like. However, a more precise analysis reveals several important differences and permits a deeper insight into the microscopic aspects of the reaction.

The reactant geometry (Figure 5a) shows that, as anticipated, the $(OH)^-\cdot 2H_2O$ cluster orients itself toward the nitromethane molecule in such a way that one of the methyl group hydrogens is directed toward the free electron pair of the hydroxide anion oxygen; this orientation facilitates the proton transfer. In comparison with the reaction with $n = 0$, the transferring proton is slightly less positive while the corresponding O−H hydrogen bond and C−H bond are *more* and *less* stretched, respectively; also, the C−N bond is a bit more stretched. The reason for these features is that the hydroxide anion solvation by the two waters is stronger than its attraction to the proton ultimately to be transferred; when the solvent is absent only one hydrogen bridge is formed (with the transferring proton). Note that other complexes can exist as a result of the interaction between the $(OH)^-\cdot 2H_2O$ cluster and the nitromethane molecule. Although an exhaustive search of the potential energy surface has not been performed, it seems that the minimum energy structure shown in Figure 5a is a reasonable starting point for the intramolecular proton-transfer reaction studied in this work. In this sense, that structure has been considered to be the reactant of the process.

In the product (Figure 5c), all three water molecules have migrated to solvate the nitro group, although only two remain in the first solvation shell (one of them being the water formed by the proton transfer). The consequences for the geometry are a very small increment in the N−O bond lengths with respect to the product for the $n = 0$ reaction, as well as a slight decrease in the C−N bond length. A principal difference with respect

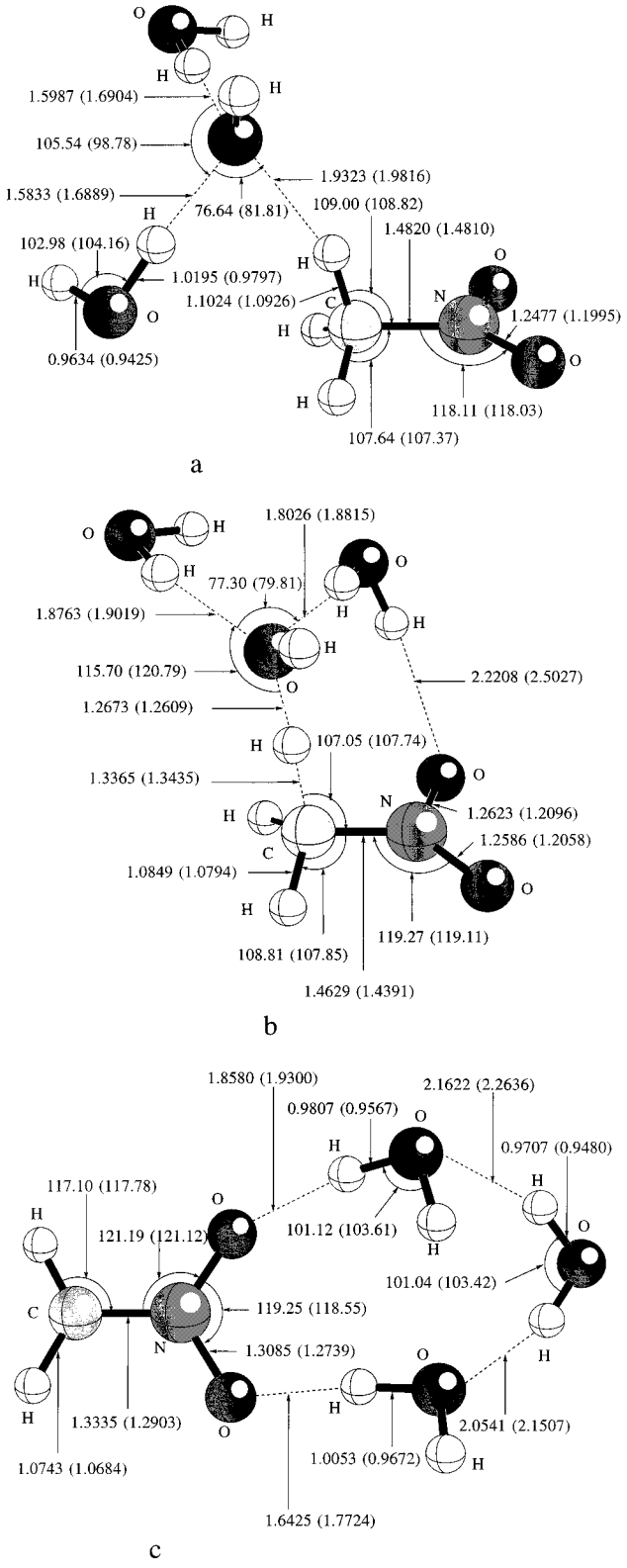

Figure 5. $NO_2CH_3 + (OH)^-\cdot 2H_2O \rightarrow (NO_2CH_2)^- + 3H_2O$ MP2 geometries: (a) reactant, (b) transition state, and (c) product; distances in angstroms, angles in degrees; RHF results in parentheses.

to the $n = 0$ reaction is noticeable in the transition state (Figure 5b). The presence of the two waters evidently shifts it away from the reactant structure: the distance between carbon and the transferring proton increases by 0.25 Å (as opposed to 0.11 Å in the $n = 0$ reaction) and the negative charge on carbon is approximately 0.05 au larger in magnitude than in the $n = 0$ reaction. The first observation is clearly in accord with the Hammond postulate (the reaction exothermicity has decreased and the energy barrier has increased), while the second one indicates the heterolytic character of the C−H bond breaking (in which carbon becomes more negative and hydrogen more positive due to solvation). Further, there has been significant motion of the solvation waters in reaching the transition state. It is also worth noting that the negative charge on carbon already begins its migration toward the nitro group as the transition state is formed (it increases in magnitude by 0.1 au), so the reaction cannot be properly considered as a two phase process (proton transfer preceding the electronic charge redistribution); rather, the two events proceed almost simultaneously.

TABLE 4: Natural Orbital Population (in au) Data for the $NO_2CH_3 + (OH)^-\cdot 2H_2O \rightarrow (NO_2CH_2)^- + 3H_2O$ Reaction[a]

structure	reactant	transition state	product
charge on carbon	−0.492, −0.532	−0.633, −0.618	−0.377, −0.390
charge on NO_2	−0.353, −0.335	−0.448, −0.482	−0.963, −0.905
charge on $(OH)^-$	−0.874, −0.784	−0.777, −0.673	
charge on H to transfer	0.343, 0.327	0.453, 0.402	

[a] First values are the RHF results, while second ones are MP2 results.

To conclude the analysis of the RHF results, one can examine the energetics of the $n = 2$ reaction in order to deduce, by comparison with its $n = 0$ counterpart, the effects of the additional water molecules. The energy barrier has clearly increased, compared to the reaction in the absence of the solvent waters: it is now equal to 7.53 kcal/mol. This is clearly consistent with the above-mentioned shift in the transition state position (in accord with the Hammond postulate), evident by inspection of the geometry optimization results. As for the reaction thermodynamics, the reaction is still exothermic, but the exothermicity is now only 14.47 kcal/mol, i.e., about half the $n = 0$ value. This, too, is an expected result in view of the anticipated better solvation of the smaller reactant hydroxide anion compared to the larger and more charge diffuse product $(NO_2CH_2)^-$ ion.

Using the optimized RHF geometries as starting points, the reactant, transition state, and product of the $NO_2CH_3 + (OH)^-\cdot 2H_2O \rightarrow (NO_2CH_2)^- + 3H_2O$ reaction were next relocated on the MP2 level. The respective geometrical parameters are also indicated in Figure 5, while the NBO populations are given in Table 4. These results are now discussed. A comparison of the geometrical and NBO population results from these MP2 level calculations with the RHF results shows that the inclusion of electron correlation does not alter significantly the reactant structure, although small variations are noticeable. A small increase of the C−H and the N−O bond distances takes place. The distances from the hydroxide anion to the transferring proton and to the water hydrogens are all reduced. The MP2 product structure is also qualitatively similar to its RHF counterpart. The trends in the observed variations are the same as in the reactant case: the intramolecular distances in the $(NO_2CH_2)^-$ anion increase, while the intermolecular distances to the water molecules that solvate the nitro group decrease.

The most apparent difference between the RHF and MP2 level results shows up in the transition state. Several aspects indicate that the MP2 transition state is further advanced toward the product: the NO_2 group is more negative (−0.482 au vs −0.448 au), the hydroxide is less negative (−0.673 au vs −0.777 au) mostly at the expense of the transferring proton (0.402 au vs 0.453 au), and the solvent waters are rotated in such a way that one of them approaches one of the NO_2 group oxygens

(2.22 Å distance). However, the distances of the transferring proton with respect to carbon and OH oxygen are not significantly changed (less than 0.01 Å change), which indicates that the contribution of the solvent water movement to the reaction coordinate is more significant when correlation is taken into account. The carbon NBO population is now −0.618 au, greater than the one corresponding to the product (−0.390 au). This type of charge distribution behavior is the same as that already found above for the $n = 0$ reaction.

Finally, the energy results obtained from the MP2 level calculations deserve attention. It was stated above that the MP2 transition state is *farther away* from the reactants or at least close to its RHF position if only the carbon-transferring proton distance is considered. A simple deduction from the Hammond postulate would then lead to the conclusion that the energy barrier should be greater or equal when correlation is included. However, this is *not* the case, as the MP2 energy barrier amounts to 3.97 kcal/mol, compared to 7.53 kcal/mol from the RHF calculations. The overall exothermicity of the reaction is also reduced by about a factor of 2 (−6.74 vs −14.47 kcal/mol). As a matter of fact, it is well-known[45−49] that the MP2 correlation correction to the energy generally reduces the proton-transfer energy barriers, as is the case here.

6. $CNCH_3 + (OH)^- \rightarrow (CNCH_2)^- + H_2O$ Reaction

As noted in the Introduction, the $CNCH_3$ molecule can provide an interesting comparison with respect to NO_2CH_3. The acetonitrile deprotonation by hydroxide has been a subject of several experimental studies, especially measuring the reaction rate,[52−54] for which a theoretical prediction is also known.[55] Exothermic proton transfer has been proposed[52] as its mechanism, with the exothermicity of about −18 kcal/mol and with essentially no temperature dependence of the rate, indicating a very low or zero energy barrier.

Our results show that the energy barrier is quite low (2.17 kcal/mol) on the RHF level and is again decreased (to 0.27 kcal/mol) when the electron correlation is included. Qualitatively, this is very similar to the case of nitromethane, with a slightly higher energy barrier and an important decrease in overall exothermicity (−10.04 kcal/mol on the RHF level, −5.46 kcal/mol on the MP2 level). These data refer to the energy difference between the reactant and product cluster structures; if one considers the separated fragments' reactant and product structures, the exothermicity is −17.98 kcal/mol on the RHF level and −9.88 kcal/mol on the MP2 level, qualitatively comparable to the experimental result.[52] Geometries of the reactant, transition state, and product are shown in parts a, b, and c of Figure 6, respectively, while the relevant NBO populations are given in Table 5. It must be remarked that a secondary product minimum exists, with the formed water molecule migrated over toward the nitrogen atom (analogous to the case of nitromethane) and with the RHF energy 0.71 kcal/mol higher than the structure of Figure 6c.

For the sake of brevity, from now on in this reaction we will only present the MP2 results. In the reactant, the oxygen atom forms a relatively strong hydrogen bond (1.63 Å O−H bond length) with one of the methyl group hydrogens, and as a consequence the corresponding H−C bond is stretched out (1.15 vs 1.09 Å for the other H−C bonds). The electronic charge transfer from $(OH)^-$ to $CNCH_3$ is notable (0.112 au). In the product structure, the resulting water molecule remains in the vicinity of the methyl group carbon atom, and it is strongly polarized. This is evidenced by the difference in the O−H bond lengths (1.01 and 0.96 Å), where the first value refers to the hydrogen that is closer to the $(CNCH_2)^-$ anion.

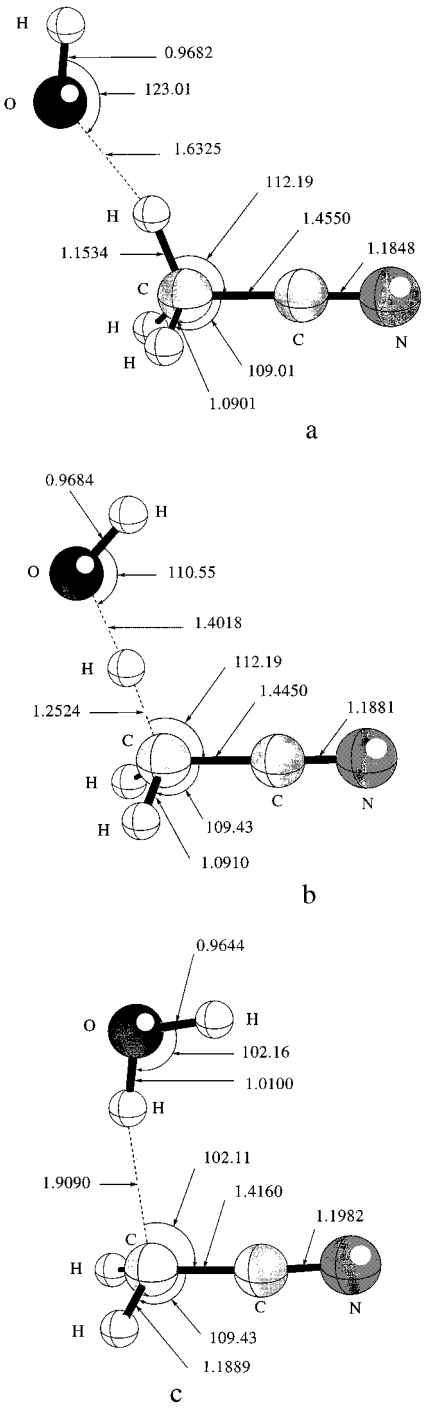

Figure 6. $CNCH_3 + (OH)^- \rightarrow (CNCH_2)^- + H_2O$ MP2 geometries: (a) reactant, (b) transition state, and (c) product; distances in angstroms and angles in degrees.

TABLE 5: MP2 Natural Orbital Populations (in au) Data for the $CNCH_3 + (OH)^- \rightarrow (CNCH_2)^- + H_2O$ Reaction

structure	reactant	transition state	product
C (CH_3)	−0.854	−0.905	−1.036
CH_3 group[a]	0.014	−0.433	−0.601
CN group	−0.126	−0.165	−0.306
H to transfer[b]	0.382	0.395	0.504
$(OH)^-$ anion[b]	−0.888	−0.797	−0.597

[a] CH2 group in transition state and in product structure. [b] These form H_2O in product structure.

The transition state geometry shows a clear similarity with the reactant. The C−C−N bond lengths remain virtually unchanged, while the H−C bond length (of the transferring

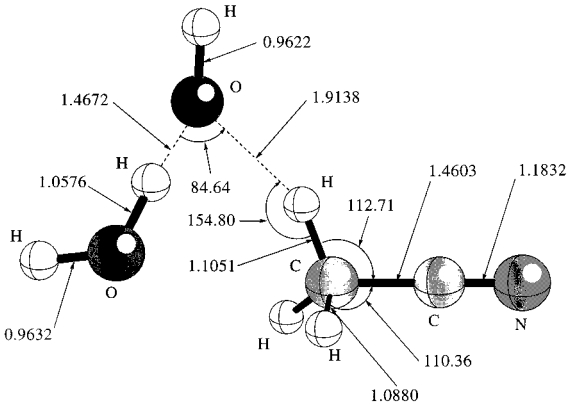

Figure 7. MP2 geometry of the cluster $CNCH_3 \cdot (OH)^- \cdot H_2O$; distances in angstroms and angles in degrees.

proton) is slightly increased from 1.15 to 1.25 Å and the C−O distance (referring to the methyl group carbon) is reduced from 2.77 Å in the reactant structure to 2.65 Å. The charge on the hydroxide anion is −0.797 au (compared to −0.888 au in the reactant) and it is transferred principally to the methyl group carbon (−0.905 au, compared to −0.854 au in the reactants). The evident reactant-like character of the transition state agrees with the reaction exothermicity, as predicted by the Hammond postulate.

A comparison of the acetonitrile and nitromethane deprotonations by the $(OH)^- \cdot nH_2O$ clusters reveals at first sight an important difference in the geometries of the product structures. In the case of nitromethane, for $n = 0$ and 2, all $n + 1$ water molecules in the product are situated around the NO_2 group, solvating the two oxygen atoms. In the case of acetonitrile, for $n = 0$, there is a stable conformation with the water molecule close to the nitrogen atom, but the energetically favorable arrangement is that in which the water molecule remains close to the methyl group carbon and solvates its electron pair. It is interesting to note that if an additional water molecule is present, i.e., $n = 1$, the calculations indicate that there is a stable reactant structure (see Figure 7) but no product minimum in which the two water molecules remain bonded with the $(CNCH_2)^-$ anion. What is found instead is that the $(CNCH_2)^-$ anion forms a cluster with the water molecule formed by the transferred proton and $(OH)^-$, while the other water molecule drifts away from the anion−water cluster. This is consistent with experimental results[52] and it is due to the fact that the CN group can accept substantially less negative charge than the NO_2 group, which is evident from the inductive Hammett parameters for standard reactions that are 0.56 for CN and 0.65 for NO_2.[56]

The final point of comparison is the negative charge on the methyl group carbon atom in all of the stationary points. In the case of nitromethane, the methyl C is more negative in the transition state than in the product (cf. sections 4 and 5), and the difference is increased for $n = 2$, when the two additional water molecules solvate the $(NO_2CH_2)^-$ anion; such behavior can cause the anomalous Brønsted parameter values. The trend is the opposite in the case of acetonitrile: −0.854 au to −0.905 au to −1.036 au, from the reactant, to the transition state, and to the product. Although the experiments on the $CNCH_3$ deprotonation by $(OH)^- \cdot nH_2O$[52,53] do not report the values of the Brønsted parameter, our results suggest that no anomalous behavior would be found.

7. Concluding Remarks

In this work we have presented a quantum chemical study of the proton-transfer reaction from nitromethane to both the hydroxide anion and the hydroxide anion clustered with two water molecules. These calculations are of particular interest in connection with the anomalous values of the Brønsted parameter in the deprotonation of certain carbon acids. In particular, they are of interest in the context of the so-called "nitroalkane anomaly",[11,12] in which the Brønsted parameter connecting the activation and reaction free energy lies outside of the expected range of zero unity; i.e., the effect of substituents on the reaction rate is not found to be intermediate to their effect on the equilibrium constant for the overall reaction. While we have not studied the Brønsted parameter itself, our studies give some insight into the role of the character of the charge redistribution often invoked[15,44] as an important ingredient for the anomalous behavior.

A natural bond orbital electronic population analysis for both the $NO_2CH_3 + (OH)^- \rightarrow (NO_2CH_2)^- + H_2O$ reaction and the $NO_2CH_3 + (OH)^- \cdot 2H_2O \rightarrow (NO_2CH_2)^- + 3H_2O$ reaction demonstrates that an important electronic charge redistribution accompanies the nitromethane deprotonation: a considerable negative charge delocalization from a relatively small hydroxide anion to a much larger $(NO_2CH_2)^-$ anion takes place. Up to the transition state, the electronic charge is transferred from the hydroxide to both the carbon atom and the nitro group. Then, as the reaction proceeds toward the product, the electronic charge migrates essentially toward the nitro group. As a consequence, the carbon negative charge at the transition state is greater than the one corresponding to the product. The opposite behavior is found for the nitro group. Our results support in a general way those previous works[15,44] that stress the importance of the differing negative charges on carbon in the transition state and in the product. In particular, they are consistent with the expectations from the valence bond theory description of the nitromethane deprotonation: two valence bond configurations (the negative charge being concentrated on carbon atom in one of them but on the nitro group oxygen atoms in the other one) make a contribution to the transition state, whereas only one configuration (with the negative charge accumulated on the nitro group oxygen atoms) is important in the product. Since the electronic description of the transition state (which determines the reaction rate) is different from the one corresponding to the product (which determines the thermodynamic properties), it is not surprising that the effect of substituents be qualitatively different at the transition state from the effect at the product, so leading to anomalous values of the Brønsted parameter.

The comparative analysis of the $CNCH_3 + (OH)^- \rightarrow (CNCH_2)^- + H_2O$ reaction strongly suggests that a critical factor for the nitroalkane anomaly is the strong electron affinity of the NO_2 group, which comes into play when the product anion is microsolvated by the surrounding water molecules. As a consequence, the methyl group carbon atom remains less negative in the product than in the transition state, and the anomalous Brønsted behavior appears. On the contrary, the CN group cannot accept so much negative charge, so as the reaction progresses toward the product, it remains chiefly on the methyl group carbon, a normal behavior of the Brønsted parameter being expected for the $CNCH_3$ deprotonation.

The initial study of microsolvation effects via the reaction involving $(OH)^- \cdot (H_2O)_2$ indicates that a first important effect of solvation is a reduction in the reaction exothermicity and the generation of an energy barrier, related to the differing solvation of the small hydroxide anion and the larger and more charge delocalized $(NO_2CH_2)^-$ anion. In addition, motion of the solvating waters is required to reach the transition state,

with even more extensive solvating water reorganization occurring subsequently to produce the products. It would be of interest in future work to systematically study larger clusters, both to trace the evolving patterns of the solvent rearrangement and to explore quantitatively the Brønsted parameter in a well-defined series of cluster reactions, which might also be studied experimentally.

In the foregoing analysis, we have described the transition state of the proton-transfer reaction in traditional classical terms, i.e., in terms of the saddle point on the potential energy surface. In an alternate quantum treatment, the proton motion would be quantized and in the bulk solution level this can lead to an alternate picture of a proton-transfer reaction.[57−60] In addition, the theoretical framework to examine the detailed applicability of the qualitative Pross three valence bond configuration picture briefly discussed in section 4 is now in place.[60] Finally, it would be of interest to conduct studies analogous to the present ones with a base weaker than OH^-, such that the nonsolvated reaction would have a well-defined and unambiguous transition state and energy barrier; this would allow a quantitative study of the Brønsted rate constant−equilibrium constant behavior as a function of increasing solvation of the base. These issues will be explored in future work.

Acknowledgment. D.B. acknowledges financial support from the "Generalitat de Catalunya" through a PIEC Fellowship no. SGR95-00401. The collaboration of J.T.H. was made possible through the Visiting Professors' Program of the IBERDROLA foundation. J.T.H. also acknowledges support from the US National Science Foundation (NSF) Grants CHE-9312267 and CHE-9700419. Financial support from DGES through Project No. PB95-0637 and the use of the computational facilities of the "Centre de Computació i de Comunicacions de Catalunya" are also gratefully acknowledged.

References and Notes

(1) Bell, R. P. *The Proton in Chemistry*; Cornell University Press: Cornell, NY, 1973.
(2) Caldin, E., Gold, V., Eds. *Proton-Transfer Reactions*; Chapman and Hall: London, 1975.
(3) Westheimer, F. H. *Chem. Rev.* **1961**, *61*, 265.
(4) Hibbert, F. *Adv. Phys. Org. Chem.* **1986**, *22*, 113.
(5) Hibbert, F. *Adv. Phys. Org. Chem.* **1990**, *26*, 255.
(6) Jencks, W. P. *Catalysis in Chemistry and Enzymology*; Dover: New York, 1987.
(7) Müller, A., Ratajczak, H., Junge, W., Diemann, E., Eds. *Electron and Proton Transfer in Chemistry*; Elsevier: New York, 1992.
(8) Truhlar, D. G. In *Rates and Mechanisms of Reactions*, 4th ed.; Bernasconi, C. F., Ed.; John Wiley & Sons: New York, 1986.
(9) More O'Ferrall, R. A. In *Proton-Transfer Reactions*; Caldin, E., Gold, V., Eds.; Chapman and Hall: London, 1975.
(10) Eigen, M. *Angew. Chem., Int. Ed. Engl.* **1964**, *3*, 1.
(11) Bordwell, F. G.; Boyle, W. J., Jr.; Hautala, J. A.; Yee, K. C. *J. Am. Chem. Soc.* **1969**, *91*, 4002.
(12) Bordwell, F. G.; Boyle, W. J., Jr.; Yee, K. C. *J. Am. Chem. Soc.* **1970**, *92*, 5926.
(13) Bordwell, F. G.; Boyle, W. J., Jr. *J. Am. Chem. Soc.* **1972**, *94*, 3907.
(14) Agmon, N. *J. Am. Chem. Soc.* **1980**, *102*, 2164.
(15) Pross, A. *Adv. Phys. Org. Chem.* **1985**, *21*, 166.
(16) Kresge, A. J. *J. Am. Chem. Soc.* **1970**, *92*, 3210.
(17) Kresge, A. J. *Chem. Soc. Rev.* **1973**, *2*, 475.
(18) Kresge A. J. *Can. J. Chem.* **1974**, *52*, 1897.
(19) Kresge A. J. In *Proton-Transfer Reactions*; Caldin, E., Gold, V., Eds.; Chapman and Hall: London, 1975.
(20) Bernasconi, C. F. *Acc. Chem. Res.* **1987**, *20*, 301.
(21) Bernasconi, C. F. *Acc. Chem. Res.* **1992**, *25*, 9.
(22) Bernasconi, C. F. *Adv. Phys. Org. Chem.* **1992**, *27*, 116.
(23) Bernasconi, C. F.; Wenzel, P. J.; Keeffe, J. R.; Gronert, S. *J. Am. Chem. Soc.* **1997**, *119*, 4008.
(24) Leffler, J. E.; Grünwald, E. *Rates and Equilibria of Organic Reactions*; John Wiley & Sons: New York, 1963; pp 156−7.
(25) Hammond, G. S. *J. Am. Chem. Soc.* **1955**, *77*, 334.
(26) Keeffe, J. R.; Morey, J.; Palmer, C. A.; Lee, J. C. *J. Am. Chem. Soc.* **1979**, *101*, 1295.
(27) Marcus, R. A. *J. Am. Chem. Soc.* **1969**, *91*, 7224.
(28) Fuchs, R.; Lewis, E. S. In *Investigation of Rates and Mechanisms of Reactions*, 3rd ed.; Lewis, E. S., Ed.; John Wiley & Sons: New York, 1974; Part 1.
(29) Roothaan, C. C. J. New Developments in Molecular Orbital Theory. *Rev. Mod. Phys.* **1951**, *23*, 69.
(30) Hehre, W. J.; Ditchfield, R.; Pople, J. A. *J. Chem. Phys.* **1972**, *56*, 2257.
(31) Hariharan, P. C.; Pople, J. A. *Theor. Chim. Acta* **1973**, *28*, 213.
(32) Clark, T.; Chandrasekhar, J.; Spitznagel, G. W.; Schleyer, P. von R. *J. Comput. Chem.* **1983**, *4*, 294.
(33) Möller, C.; Plesset, M. S. *Phys. Rev.* **1934**, *46*, 618.
(34) Schlegel, H. B. *J. Comput. Chem.* **1982**, *3*, 214.
(35) Frisch, M. J.; Trucks, G. W.; Schlegel, H. B.; Gill, P. M. W.; Johnson, B. G.; Robb, M. A.; Cheeseman, J. R.; Keith, T. A.; Petersson, G. A.; Montgomery, J. A.; Raghavachari, K.; Al-Laham, M. A.; Zakrzewski, V. G.; Ortiz, J. V.; Foresman, J. B.; Cioslowski, J.; Stefanov, B. B.; Nanayakkara, A.; Challacombe, M.; Peng, C. Y.; Ayala, P. Y.; Chen, W.; Wong, M. W.; Andres, J. L.; Replogle, E. S.; Gomperts, R.; Martin, R. L.; Fox, D. J.; Binkley, J. S.; Defrees, D. J.; Baker, J.; Stewart, J. P.; Head-Gordon, M.; González, C.; Pople, J. A. Gaussian 94 (Version B.3); Gaussian Inc.: Pittsburgh, PA, 1995.
(36) McKee, M.. *J. Am. Chem. Soc.* **1985**, *107*, 1900.
(37) Lammertsma, K.; Prasad, B. V.. *J. Am. Chem. Soc.* **1993**, *115*, 2348.
(38) Tannenbaum, E.; Johnson, R. D.; Myers, R. J.; Gwynn, W. D. *J. Chem. Phys.* **1954**, *22*, 1949.
(39) Tannenbaum, E.; Johnson, R. D.; Myers *J. Chem. Phys.* **1956**, *25*, 42.
(40) Trevino, S. F.; Prince, E.; Hubbart, C. R. *J. Chem. Phys.* **1980**, *73*, 2996.
(41) Carrigan, K. E. M.S. Thesis, University of Colorado, Boulder, CO; unpubl. 1984.
(42) Newton, M. D.; Ehrenson, S. *J. Am. Chem. Soc.* **1971**, *93*, 4971.
(43) Tuñón, I.; Rinaldi, D.; Ruiz-López, M. F.; Rivail, J. L. *J. Phys. Chem.* **1995**, *99*, 3798.
(44) Pross, A.; Shaik, S. S. *J. Am. Chem. Soc.* **1982**, *104*, 1129.
(45) Cybulski, S. M.; Scheiner, S. *J. Am. Chem. Soc.* **1987**, *109*, 4199.
(46) Szczesniak, M. M.; Scheiner, S. *J. Chem. Phys.* **1987**, *77*, 4586.
(47) Cybulski, S. M.; Scheiner, S. *J. Am. Chem. Soc.* **1989**, *111*, 23.
(48) Bosch, E.; Moreno, M.; Lluch, J. M.; Bertrán, J. *Chem. Phys.* **1990**, *148*, 77.
(49) Paz, J. J.; Moreno, M.; Lluch, J. M. J. *J. Chem. Phys.* **1995**, *103*, 353.
(50) Yamdagni, R.; Kebarle, P. *J. Am. Chem. Soc.* **1971**, *94*, 2940.
(51) Larson, J. W.; McMahon, T. B. *J. Am. Chem. Soc.* **1983**, *105*, 2944.
(52) Yang, X.; Zhang, X.; Castleman, A. W., Jr. *J. Phys. Chem.* **1991**, *95*, 8520.
(53) Mackay, G. I.; Betowski, L. D.; Payzant, J. D.; Schiff, H. I.; Bohme, D. K. *J. Phys. Chem.* **1976**, *80*, 2919.
(54) Hierl, P. M.; Ahrens, A. F.; Henachman, M.; Viggiano, A. A.; Paulson, J. F. *J. Mass Spectrosc. Ion Processes* **1987**, *81*, 101.
(55) Su, T.; Chesnawitch, W. J. *J. Chem. Phys.* **1982**, *76*, 5183.
(56) March, J. *Advanced Organic Chemistry*, 4th ed.; John Wiley & Sons: New York, 1992; p 283.
(57) Borgis, D.; Hynes, J. T. *J. Chem. Phys.* **1991**, *94*, 3619.
(58) Staib, A.; Borgis, D.; Hynes, J. T. *J. Chem. Phys.* **1995**, *102*, 2487.
(59) Ando, K.; Hynes, J. T. *J. Mol. Liq.* **1995**, *64*, 25.
(60) Bianco, R.; Hynes, J. T. *J. Chem. Phys.* **1995**, *102*, 7864.